Separation and Purification Technology 376 (2025) 134073

Contents lists available at ScienceDirect

Separation and Purification Technology

journal homepage: www.elsevier.com/locate/seppur

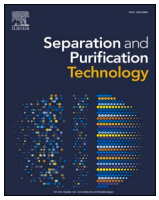

Separation of carboxylates using electrodialysis: a key process for the electro-refinery concept

M. Richa, R. García-Cervilla, J. Lobato, P. Cañizares, M.A. Rodrigo *

Department of Chemical Engineering, Faculty of Chemical Sciences & Technologies, University of Castilla-La Mancha, Campus Universitario S/n., 13071 Ciudad Real, Spain

ARTICLE INFO

Keywords:
Electrodialysis
Carboxylates
Purification
Separation
Electro-crystallization

ABSTRACT

Electrodialysis, using anion exchange membranes, is an effective technique for separating carboxylates in aqueous solutions. By leveraging the different pKa values of acids, selective separation can be achieved, enhancing the value of the aqueous streams. Thus, electrodialysis can serve as both a separation and purification method. In this work, the transport of carboxylates (oxalate and acetate) through four types of commercial anion exchange membranes (AEMs) has been evaluated. The main characteristics of this transport, particularly those relevant to the purification of streams necessary for the development of electro-refining processes of organic products, have been determined. Significant differences were observed among the membranes, with Fumasep FAB-PK-130 showing the highest efficiency in separating oxalate through electrochemically assisted crystallization, achieving 50% crystallization of oxalic acid in under 10 h. Additionally, pH control enabled the separation of oxalates and acetates, resulting in an aqueous stream containing only oxalic acid from an equimolar mixture of oxalic and acetic acids. However, the results are quite different from those expected according to the acid-base equilibrium of bulk solution that relates the dissociated ionic species and protonated molecular species in both compounds. This highlights the existence of local pH profiles that influence this separation and that need to be understood to achieve effective purification.

1. Introduction

Developing environmental applications to tackle wastewater discharge, especially with organic contaminants, has been a key research objective for decades [1–5]. The immediate solution sought has been the complete mineralization of organic compounds into carbon dioxide [6–12]. Various processes, from biological to advanced oxidation techniques, have been developed to achieve this goal. Climate change, resource needs due to population growth, and rising living standards have motivated the biorefinery concept as an alternative treatment [13–15]. This approach uses biological processes to transform organic compounds into valuable materials and energy resources, minimizing carbon dioxide generation. It applies to various wastes, not just wastewater. Technological advancements enable a more sustainable world beyond traditional treatments. The biorefinery concept has driven research in other environmental fields, prioritizing circular economy and sustainability, especially regarding the carbon footprint [15–19].

Environmental electrochemical technology has been pursuing this goal for years, developing its potential with increasingly efficient processes in terms of selectivity and energy consumption [8,15,20,21]. In the first case, the development of processes with high faradaic efficiency has been prioritized, meaning that, especially through the development of suitable electrodes, the electrons involved are used in the desired reactions [8,22–24]. Also, integrating anodic and cathodic processes so that the same electrons obtained in the reductive process of interest are used in the oxidative process of interest. In the second case, with the design of cells that allow lowering the cell voltage by minimizing ohmic drops [25]. Also, with the direct supply of renewable energy, demonstrating that the electrochemical process practically only requires electricity, which can be obtained sustainably [26–28]. The electro-refinery concept mimics biorefinery success using electrochemical processes, combining oxidative electrolytic transformation of pollutants with electrodialysis and organic electrosynthesis for purification and valorization. This concept has multiple development possibilities, as outlined in a recent review [29].

This technological approach is feasible because the oxidative degradation of any organic compound involves an intermediate phase preceding mineralization, during which the compound is converted into

* Corresponding author.
E-mail address: manuel.rodrigo@uclm.es (M.A. Rodrigo).

https://doi.org/10.1016/j.seppur.2025.134073
Received 19 February 2025; Received in revised form 5 May 2025; Accepted 20 June 2025
Available online 21 June 2025
1383-5866/© 2025 The Authors. Published by Elsevier B.V. This is an open access article under the CC BY-NC-ND license (http://creativecommons.org/licenses/by-nc-nd/4.0/).

carboxylates [15,30]. This transformation is not exclusive to electrochemical processes, as oxidation in most technologies (including even biological treatments) occurs by the insertion of oxygenated groups that sequentially lead to alcohols, ketones, aldehydes, and carboxylic acids, along with the breaking of aromatic or aliphatic chains. The important issue about electrochemical technology is that by selecting the electrocatalytic anode material and operating conditions (especially current density or cell voltage), the composition of carboxylic acids can be controlled, directing the process towards compositions of interest [30].

The separation of organic compounds in aqueous solutions can be tackled by different technologies. However, there is a technique with particularly good characteristics, which is electrodialysis, through which carboxylates can be separated using anion exchange membranes [31,32]. Not only this, but by using the different pKa values associated with the different acids, a selective separation could even be achieved, significantly increasing the added value of the generated aqueous streams. In other words, electrodialysis could, in principle, be used as a separation and purification technique.

In this work, two carboxylic acids were selected as a model. These acids were oxalic acid (OA) and acetic acid (AA). These acids have been observed to be produced mostly, among other acids, by oxidizing organic matter in previous work [33]. Moreover, these carboxylates are among the most commonly present in primary oxidative destruction processes of organic matter, enhancing the which gives the study significant added value. In this way, acetate is frequently produced during fermentative stages in numerous microbial pathways for contaminant degradation. [34,35], while oxalate is more associated with chemical degradation processes [15,36]. Particularly with the use of advanced oxidation techniques, these acids tend to accumulate in the treatment liquid due to their lower oxidizability compared to other reaction intermediates generated during contaminant degradation. Furthermore, their short two-carbon chains and distinctly separated pKa values make them suitable for investigating the feasibility of separation via electrodialysis based on pH regulation.

The ionic dissociation equilibria of these two compounds which are going to be evaluated in this work is shown in equations (1) to (3). Acetic acid has a pKa of 4.76 [20], while the second oxalic acid constant is slightly lower, around 4.26 units (depending on the bibliographic source, values between 3.81 and 4.27 are found) [20], and where there is a very significant difference is in its first ionization, with values that, according to the literature, are around 1.27 units (although again, the value depends on the reference, with values found in the range between 1.20 and 1.46) [20].

$$(COOH)_2 \leftrightarrows HOOC - COO^- + H^+ \quad (1)$$

$$HOOC - COO^- \leftrightarrows (COO^-)_2 + H^+ \quad (2)$$

$$CH_3 - COOH \leftrightarrows CH_3 - COO^- + H^+ \quad (3)$$

To evaluate the use of the proposed technology for the separation of carboxylate streams, a strategy was devised based on combining the electrodialysis treatment with a planned modification of the pH according to the different acidity constants of the carboxylic acids to be separated, since the anion exchange membrane although it can allow the passage of molecular species due to the concentration gradient (carboxylic acid) in an electric field should be favoured the migration of ionized species (carboxylate) due to electrostatic attractions towards the anode. By selecting appropriate pH values, it is possible to achieve a higher degree of dissociation for one of the compounds. This dissociated compound will pass more efficiently through the membrane, favoring the concentration of the less dissociated species in the feed compartment and the more dissociated species in the product compartment.

Given this context, the aim of this study is to assess the effectiveness of various anion exchange membranes in separating and purifying carboxylate-containing streams. The findings will be crucial for optimizing the electro-refinery concept, as this process serves as the foundation of the technology and its efficiency directly determining the added value that can be extracted from processed waste.

2. Material and methods

2.1. Membranes

Four commercially available anion exchange membranes (AEMs) were purchased from the Fuel Cell: RALEX-AMH-PEX (AMH) (from MEGA), Fumasep FAA-3-PK-130 (FAA), Fumasep FAB-PK-130 (FAB) and Fumasep FAS-PET-130 (FAS). A cation exchange membrane (CEM) was also used to separate the electrodes to the process compartment of the cell: Fumasep FKS-50 (FKS). Their main data are shown in Table SM1. These membranes were selected for their distinct properties and potential applicability in electrodialysis processes. In terms of thickness, FAA, FAB, and FAS are considerably thinner than AMH. Regarding proton transfer and ion exchange capacity, the order from highest to lowest is as follows: FAA > FAS > FAB. These properties are unknown for AMH.

2.2. Chemicals

Oxalic acid (OA) (> 99 %) and acetic acid (AA) (> 99 %) were used as model carboxylic acids and were purchased from Panreac. Sodium hydroxide ($NaOH$) (Scharlab) and sulfuric acid (H_2SO_4) (> 98 %) (Panreac) were used to adjust pH. Sulfuric acid was also used as the mobile phase in liquid chromatography. Sodium sulfate (Na_2SO_4) (Fisher) was used as catholyte and anolyte. All aqueous solutions were prepared using ultrapure deionized water (MilliQ) with a conductivity of less than 1 $\mu S \cdot cm^{-1}$.

2.3. Experimental setup

For this work, a four-compartment electrodialysis cell (Fig. 1) has been designed and manufactured using 3-D printing by

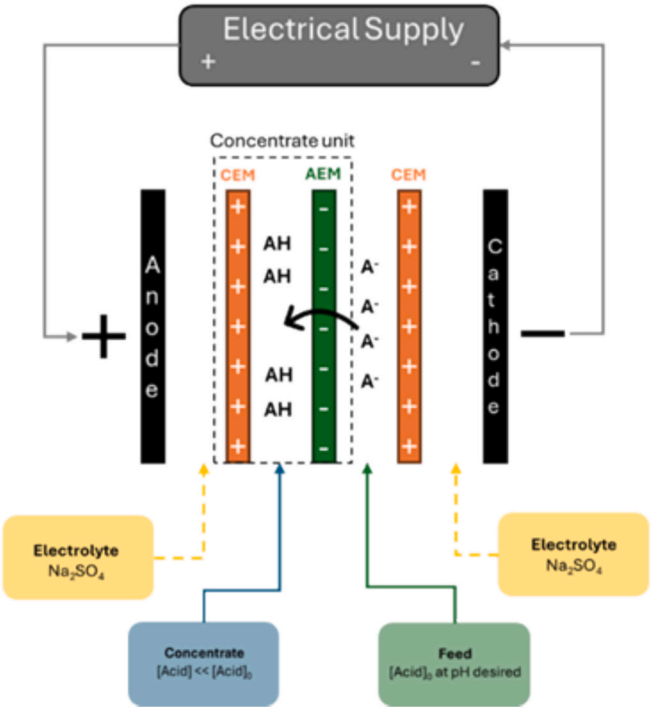

Fig. 1. Scheme of the experimental setup for the selective recovery of carboxylic acids.

stereolithography, with a special mechanical design for the inlet and outlet nozzles and a body for the electrodes, feed, and recovery compartments that generates a rotating flow from the electrolyte streams circulating in each of them, promoting high mass transfer and sufficient shear stress to prevent the formation of solid deposits on membranes or electrodes. The parts that constitute the cell have been slightly modified from those studied in previous works [37]. The cell was manufactured with a 3D printer Form 3 (Preform) and made with Clear V4 resin from Preform. It was designed with the software Autodesk® Fusion. The experimental setup consisted of four 10 mL compartments assembled in line. These compartments were the Anolyte, Catholyte, Feed and Product compartments. Each compartment was connected to a recirculating tank. A peristaltic pump (Heidolph Pumpdrive 5001) at a flow rate of 10 $mLmin^{-1}$ was used to provide the recirculation between the bottles and the different compartments of the electrodialysis cell. The Catholyte and Anolyte tanks had a volume of 150 *mL*. The feed tank 500 *mL* and the product tank 100 *mL*. These compartments were assembled in the order Anolyte – Product – Feed – Catholyte (Fig. 1). A CEM was placed between the Anolyte and Product compartments. A CEM was also placed between Feed and Catholyte. Between Product and Feed the corresponding AEM (AMH, FAA, FAB or FAS) was placed. The system utilized a mixed metal oxide (MMO) (Ti/RuO_2) as anode and a stainless-steel as cathode. The dimensions of the electrodes were 2.5 × 2.5 *cm* (the total surface was 6.25 cm^2). In the anolyte and catholyte tanks a solution with 100 mM sodium sulfate was used as the electrolyte.

2.4. Experimental procedure

2.4.1. Membrane selection experiments

The first set of experiments was conducted to characterize the behavior of the four types of AEMs (AMH, FAA, FAB, and FAS) in the transport of oxalate and acetate and to select the most suitable for the later separation of the two carboxylic acids. In the tank connected with feed compartment, a solution with the corresponding carboxylic acid was added (100 mM of OA or 500 mM of AA) and pH was adjusted at 1.5. In the tank connected with the product compartment, a solution with the corresponding acid (OA or AA) was also added, with a lower concentration than in the feed tank (10 mM), and pH was not adjusted. The experiments were conducted at two different current densities and without application of electric current (0, 12.8, and 25.6 $mAcm^{-2}$). Each run consisted of 6 h and samples were collected hourly from both the feed and product compartments and then, acid concentrations were measured. All experiments were performed in duplicate. The values shown correspond to the average of the results obtained.

2.4.2. Electrochemically assisted crystallization experiments

To study the electrochemically assisted crystallization of oxalic acid, several additional tests were carried out using the FAB AEM to separate feed and product compartments. As the feed solution (in the tank connected to the feed compartment), a solution with 100 *mM* of OA was added to the corresponding bottle and pH was adjusted to 3.0. In the product tank, a solution with a lower concentration of OA was added (10 *mM*) and pH was not adjusted. Three different current densities 12.5, 25.0 and 37.5 $mAcm^{-2}$ were applied. An additional experiment without application of current density was also carried out. The experiments were left for sufficient time to reduce the oxalic acid concentration by 80 % in the feed stream, with the aim of obtaining significant crystallization. Samples were collected at different times from feed and product tanks. All experiments were performed in duplicate. The values shown correspond to the average of the results obtained.

2.4.3. Purification experiments

To investigate the effect of the pH in the Feed compartment on the separation and purification of oxalic acid from solutions containing oxalic and acetic acid, two experiments were conducted using again the FAB AEM to separate the feed and product compartment. acetic acid (AA). The feed in the tank connected to the feed compartment consisted of a solution with 50 *mM* of each carboxylic acid (oxalic and acetic acid). The pH in the feed tank was adjusted at two different pH (1.5 and 0.6). In the tank that collects the product, a solution with 10 *mM* of oxalic acid was added and pH was not adjusted. Experiments were carried out at 25.6 $mAcm^{-2}$ of current density. Each experiment was conducted for a total duration of 6 h, with samples collected at different times from feed and product tanks to monitor acid concentrations. All experiments were performed in duplicate. The values shown correspond to the average of the results obtained.

2.4.4. Limiting current density tests

Four experiments, one with each of the AEMs (AMH, FAA, FAB and FAS) were carried out to find out whether the experiments performed in the previous sections are below or above the limit of the current density limit of the system. In the tank connected with feed compartment, a solution with the corresponding carboxylic acid was added (500 mM of OA or AA) and pH was adjusted at 1.5. In the tank connected with the product compartment, a solution with the corresponding acid (OA or AA) was also added, with a lower concentration than in the feed tank (10 mM), and pH was not adjusted. The experiments were conducted at different voltages (in a rank from 0 V to 30 V) and the resulting intensity of the system was measured. All experiments were performed in duplicate. The values shown correspond to the average of the results obtained.

2.5. Analytical methods

Conductivity measurements were performed using a GLP 31 conductivity meter, while pH was measured using a GLP 22 pH meter, both from Crison Instruments S.A. (Spain). The concentration of carboxylic acids in both the feed and concentrate compartments was determined through high-performance liquid chromatography (HPLC) using an Agilent 1100 system. The column used was Hi-plex H from Agilent. Mobile phase was H_2SO_4 100 *mM*. The temperature was 50°C and flow rate was 0.6 $mLmin^{-1}$. Samples were filtered before analysis to remove any particulate matter and prevent interferences.

2.6. Estimation of carboxylic acids dissociation

Expected values of the ionic and molecular species can be easily calculated from the values of the dissociation constants using equations (4) to (8), where Ka_1 and Ka_2 are the first and second acid dissociation constants respectively of oxalic acid. Ka_3 is the acid dissociation constant of acetic acid. C_t is the total concentration of all species in the solution for the corresponding carboxylic acid (oxalic or acetic).

$$[(COOH)_2] = \frac{C_t}{1 + \frac{Ka_1}{[H^+]} + \frac{Ka_1 Ka_2}{[H^+]^2}} \tag{4}$$

$$[HOOC - COO^-] = \frac{Ka_1[(COOH)_2]}{[H^+]} \tag{5}$$

$$[(COO^-)_2] = \frac{Ka_1[HOOC - COO^-]}{[H^+]} \tag{6}$$

$$[CH_3 - COOH] = \frac{C_t}{1 + \frac{Ka_3}{[H^+]}} \tag{7}$$

$$[CH_3 - COO^-] = \frac{Ka_3[CH_3 - COOH]}{[H^+]} \tag{8}$$

On the other hand, as shown in equation (9), when the pH is sufficiently far from the pKa value, the formation of one of the species is favored over the others, as the difference in units corresponds to the number of

logarithmic units that one species is more concentrated than the other in the resulting mixture. This should allow selective separations if the separation between the pKa of the acids is sufficiently large, although this needs to be verified experimentally in our case study.

$$\frac{[R-COO^-]}{[R-COOH]} = 10^{(pH-pK_a)} \quad (9)$$

3. Results and discussion

3.1. Selection of anion exchange membrane

A series of tests was conducted to characterize the transport of acetates and oxalates through four commercially available AEMs (AMH, FAA, FAB, and FAS), selected because of their markedly different characteristics, trying to determine which membrane has the best characteristics for separating these species. These tests were conducted for each compound separately at pH 1.5, since at this pH value the acetic acid dissociation is expected to be almost negligible (0.055 %), while oxalic acid is expected to be highly dissociated (66.143 %). This implies that the transport of ionic species through the membrane should be very different, with oxalate transport being favored over acetate at this pH, which should be practically negligible. In addition, the chosen concentrations of acetic and oxalic acid to formulate the starting solutions were selected based on previous tests, using the (arbitrary) criterion that ion transport under conditions of no electric current application should be as similar as possible for a fair comparison (this rate was achieved with the ratio of concentrations proposed).

Fig. 2 shows the variation in acetic acid amount (mmol) measured in the carboxylate product compartment over time during the six-hour duration of each test, for each of the four membranes whose performance is being evaluated in this work. Surprisingly, the transport of this compound is very significant and highly dependent on the current density applied, which indicates a high contribution of the electromigration process, despite the initial expectation based on acid-base dissociation equilibria. During the process, the pH in the compartment containing the feed solution only experiences a small increase of less than 0.3 units, so the ionization of acetic acid in the bulk is practically unaffected. This points out that the equilibrium must be shifting rapidly near the membranes to allow the transport process of the ionized species to develop efficiently and it does not limit the process rate. It is important to note that the anionic species in this compartment goes through the AEM, and the separation of carboxylate is intended. A cation exchange membrane prevents hydroxyl ions formed at the cathode be transported to the compartment. On the contrary, the charge balance in the compartment is compensated by the transport of protons through this membrane to the electrode compartment, where they do interact with these hydroxyl ions, helping to keep charge balance in all compartments.

As well, it is important to mention that the volume of the feed solution contained in the feed reservoir bottle is 5 times greater than that of the product (500 and 100 *mL*, respectively). Due to this fact, the acetic acid concentration between the two compartments is equalized after a time of, approximately, 3 – 5 *h* for the experiments where electric current was applied. From that moment, although the concentration difference between the two compartments continued to increase, the observed trend did not change. This means that acetate was forced to cross the membrane against the concentration gradient by the application of current (cathode to anode direction). Furthermore, this process was not affected by the difference in concentrations between the compartment in the observed ranges because linearity is maintained. Similarly, A. Chandra et al., [38] observed a linear recovery of citric acid with voltages in the rank 15–20 V with variations in the current density lower than 2 mA cm^{-2}.

Regarding changes during each test, it can be observed that the amount transported increases linearly with time in all the tests conducted and that, as expected, the transport rate (slope of the lines) increases with the current density applied to the system. In fact, the linear increase in transport rate observed with increasing current density indicates that the process is not being limited by the concentration of ionic species at any time during the process and confirms the shifting in the equilibrium towards the ionic species in the nearness of the membrane because, as it has been pointed out, the pH in the feed compartment does not change importantly and it is maintained in the nearness of pH 1.5

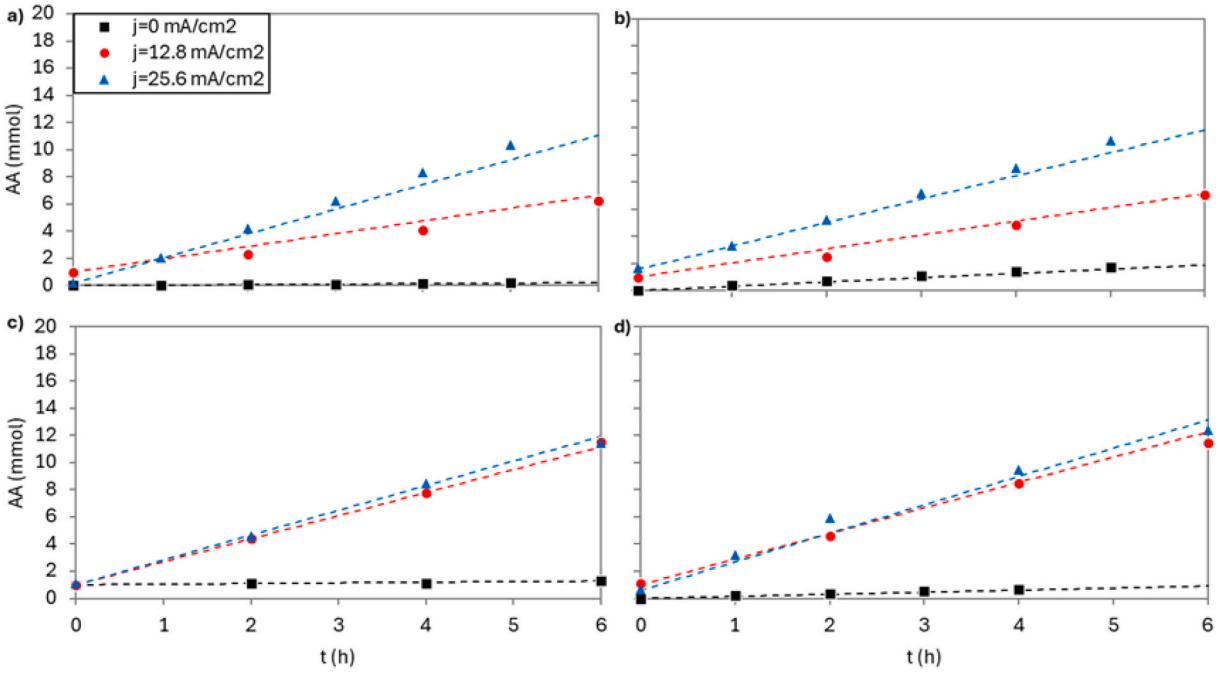

Fig. 2. Total amount of migrated acetic acid (*mmol*) from the feed compartment over the time at different current densities 0 $mAcm^{-2}$ (black squares), 12.8 $mAcm^{-2}$ (red circles), and 25.6 $mAcm^{-2}$ (blue triangles) for the four membranes: AMH (a), FAA (b), FAB (c) and FAS (d). Symbols represent experimental results and lines represent a linear fitting.

during the complete duration of the tests, conditions at which acetic acid is the primary species and acetate concentration is completely negligible.

It can also be noted that carboxylate transport depends not only on the current density but also on the type of membrane. The calculated carboxylates transport rates, *u*, are shown in Fig. 3, where it is observed that the molar migration rates of FAB and FAS membranes have similar behavior, with carboxylate transport rates that seem to stabilize in the evaluated current density range. The rates do not vary significantly with the current density between 12.8 and 25.6 mA cm^{-2}, unlike the FAA and AMH membranes, where the observed increase is linear throughout the range. For the highest current density, the FAB membrane is the one that reaches the lowest transport rate of acetate.

These trends indicate that transport is favored in the former membranes (FAB and FAS) at low current density, which initially seems advantageous for their use in carboxylate separation. Regarding the results of the tests conducted without applying electric current, it can be observed that all four membranes allow carboxylate transit by diffusion, with the FAB and AMH membranes being the least favorable for this transport mechanism and the FAA membrane the most suitable.

Similar results are obtained in the transport of oxalic acid, as shown in Fig. 4, where it can be observed again that the increase in carboxylate concentration measured in the acid product compartment is linear during the six-hour duration of the tests, and that there is also a significant effect of the membrane type and operating current density. In this case, the transport was expected since, according to the equilibrium constants and the pH in the feed compartment, nearly 67 % of the species derived from oxalic acid are in dissociated form. For this reason, it is surprising that the transport rates are comparable to those of acetate, although they are indeed somewhat higher.

Again, it is important to remind that the volume of the feed is 5 times greater than that of the product. Therefore, after 6 *h*, at 25.6 $mAcm^{-2}$ the concentration in the feed compartment in all experiments decrease between 25.7 and 38.3 % being the concentration in the product compartment 103.0 – 300.9 % higher than that of the feed compartment. Consequently, it can be concluded that, within the studied period, the migration rate of oxalic acid through the AEMs is independent of the oxalic acid concentration on both sides of the AEM. In addition, it can be added that the application of electric current lets the migration of the oxalate against the concentration gradient.

The values of the oxalic transport rates are shown in Fig. 5. When observing the effect of current density, similarities and important differences are noted compared to the case of acetic acid.

In both cases, the FAB membrane seems to offer the worst result in terms of rate, and the FAA membrane shows the highest stabilization (or saturation) in transport rate with current density, while in the other three, the rate increase is practically linear with current density. In the absence of electric current application, FAB and AMH again show less favorability for the diffusion transport mechanism, with oxalate transit being practically negligible in the absence of an electric field, as was also the case with acetate. The FAA membrane also shows the most favored transport in the absence of electric current, as was the case with acetate.

There is an important difference between the behavior of oxalate and acetate, as in several of the tests conducted, crystallization of oxalic acid is observed both on the membrane surface and in the bulk of the electrolyte (which seems to be associated with the detachment of crystals formed on the membrane). The quantification of this crystallization has been carried out by mass balance, through the difference between the decrease in carboxylate in the feed compartment and its increase in the concentration compartment solution. Although this procedure has been found to yield values similar to the separation, drying, and weighing of the crystals (this was verified with the last samples), this method based on solution measurement has been considered more reliable than gravimetric quantification, given the difficulty in collecting all the crystals throughout the installation, which affects the precision of the quantification and cannot be made during the test (as part of the crystals are inside the cell and this device cannot be opened for cleaning during the tests). Considering this, the resulting value after the six-hour duration of the tests is shown in Fig. 6, where it is observed that the crystallization process is favored when operating at high current densities and, especially, with the FAA and FAB membranes, being practically negligible with the FAS membrane. In fact, in the case of FAB, crystallization is observed even when the cell was operating at low current density, pointing out that this membrane is promoting this process.

The explanation of the crystallization process must be based on the concentration of this compound on the membrane surface, which favors the formation of seed crystals that subsequently grow in the system. It should be noted that, from the process efficiency point of view, this electrochemically assisted crystallization of oxalic acid is very advantageous, as long as it does not affect the process operation by blocking the membrane, as observed in the tests conducted, since it allows the separation of the purified species during the process, which is one of the final objectives to be achieved. The shear stress associated with the rotational flow induced by the special mechanical design of the electrolyte inlet and outlet tubing of the compartments and the compartment shape itself helps explain why no problems have been observed in this regard with the cell design used.

Another interesting point in the evaluation of the crystallization

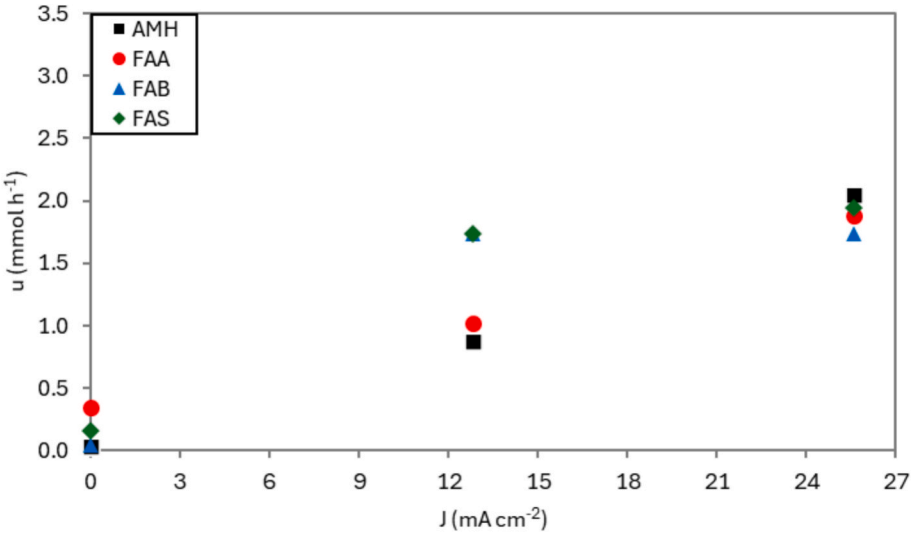

Fig. 3. Experimentally obtained molar rates, u ($mmolh^{-1}$), of acetic acid through the different membranes tested at the different current densities used.

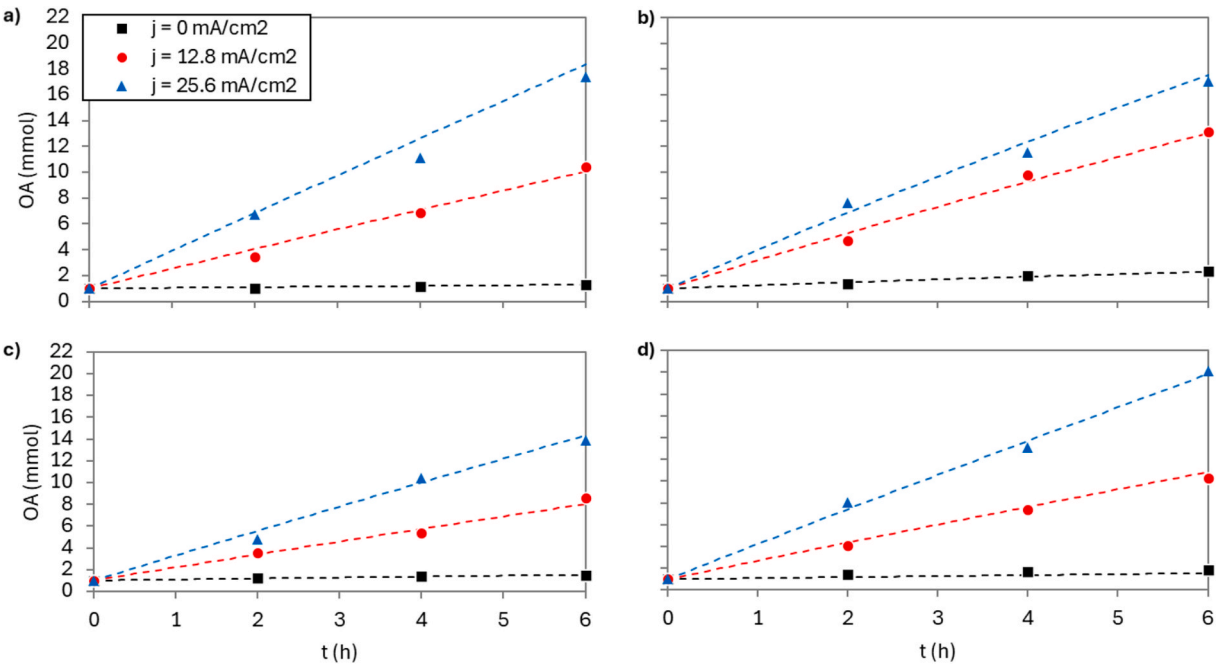

Fig. 4. Total oxalic acid migrated (*mmol*) from the feed compartment over the time at different current densities 0 $mAcm^{-2}$ (black squares), 12.8 $mAcm^{-2}$ (red circles), and 25.6 $mAcm^{-2}$ (blue triangles) for the four membranes: AMH (a), FAA (b), FAB (c) and FAS (d). Symbols represent the experimental results and lines represent a linear fitting.

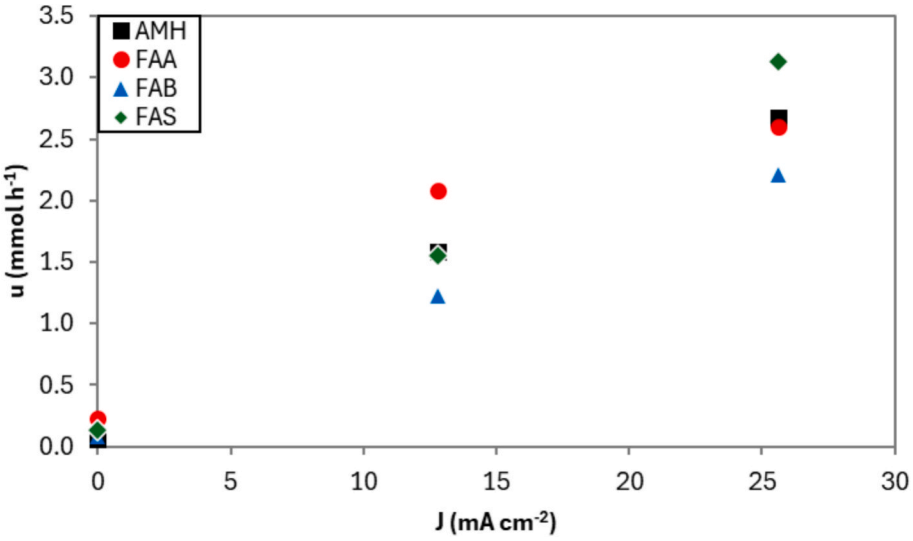

Fig. 5. Experimentally obtained molar rates, u ($mmolh^{-1}$), of oxalic acid through the different membranes tested at the different current densities used.

process is that no specific changes in the pH or conductivity in these tests are associated to the membrane used. This can be clearly seen in Fig. 7, where the evolution of pHs and ionic conductivities in the different tests made in this section are compared. As seen, the test made with the four anionic exchange membranes lead to the same patterns in both parameters that seem to be only related to the current intensity. In both compartments an increase in the pH is observed, being higher at higher current densities. This is especially important in the product compartment, and it is explained in terms of the reaction of protons formed on the anode, and transported to this compartment through the CEM, with the carboxylates that cross the membrane, as the supply of protons was expected to produce not an increase but a decrease in the pH. In the feed compartment, the increase of the pH has to be also related to the dissociation equilibria of the oxalate/oxalic acid, as the hydroxyl anions produced on the cathode are not expected to cross significantly through the CEM.

The higher OA crystallization results obtained by the FAB membrane can be explained by its greater proton blocking capacity. This characteristic should favor the formation of a more intense proton gradient on the surface of this membrane compared to the other membranes studied, which in turn promotes the generation of the initial seed crystals from which the crystallization process develops. Thus, if the catalog characteristics of this membrane are compared with those of the other membranes supplied by the same manufacturer, the values of proton transfer capacity measured by pH potential in a 0.1 M HCl / 0.1 M NaCl concentration cell at a temperature of 25 °C are less than 500 nmol min^{-1} cm^{-2} for the FAB membrane and between 800 – 2500 µmol min^{-1} cm^{-2} for the FAA and 900 – 1500 µmol min^{-1} cm^{-2} for the FAS, more than

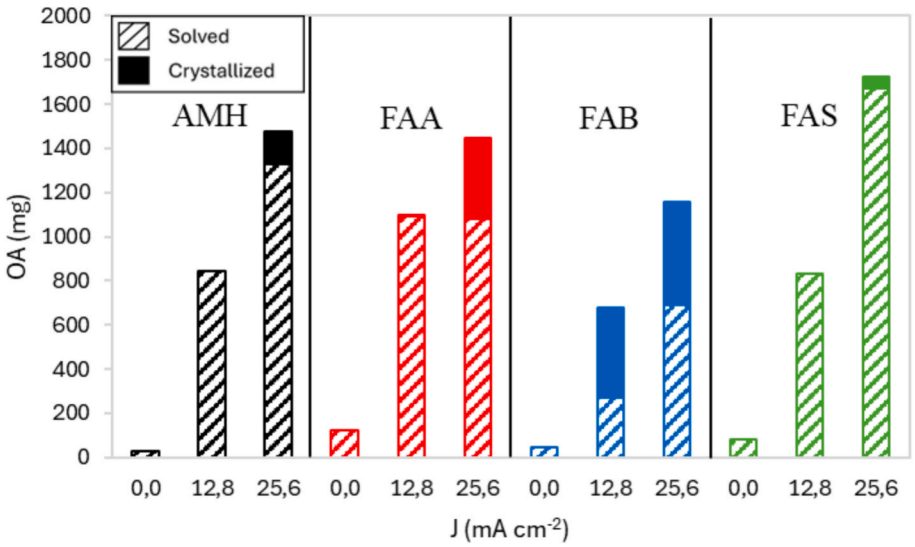

Fig. 6. Total oxalic acid migrated from the feed compartment to the product compartment in crystalline form (solid column) or dissolved within the solution (striped column) at different current densities and for the four membranes evaluated in this work.

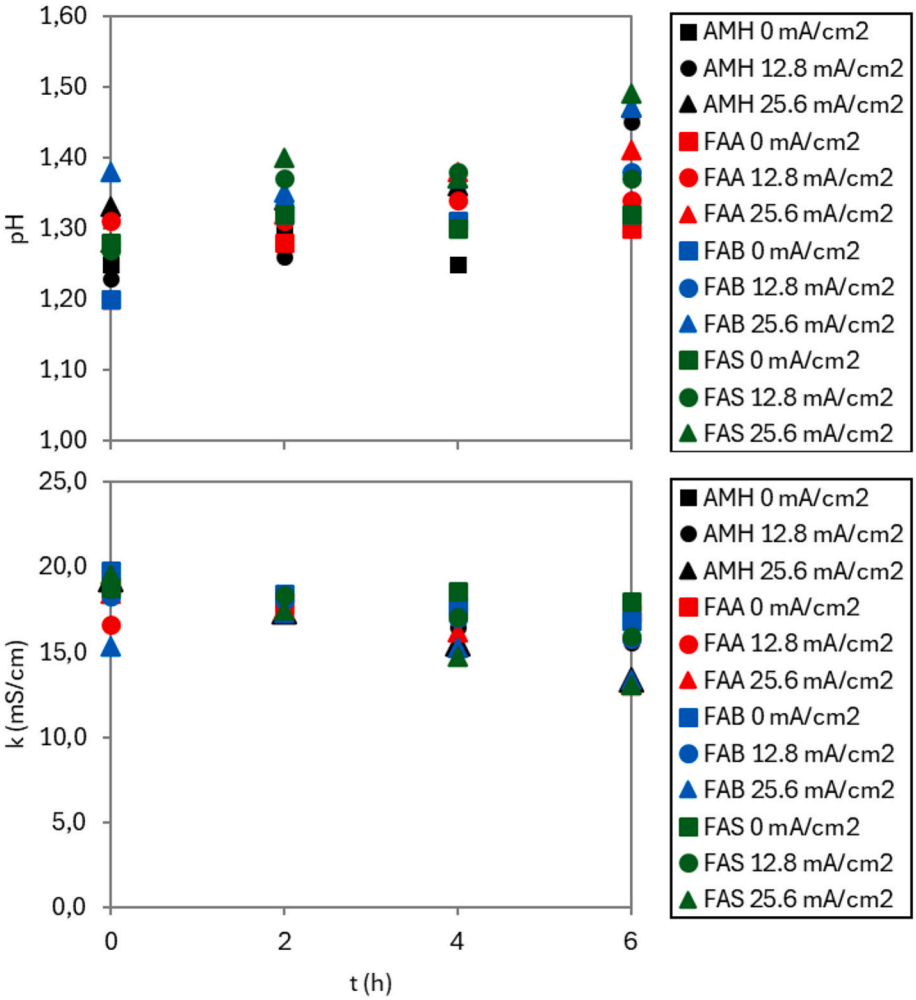

Fig. 7. Time course of pH (part a) and ionic conductivity (part b) during the tests in which the transport of oxalate through the four membranes is evaluated (feed compartment).

three logarithmic units higher.

In general terms, in the product compartment, changes in pH and conductivity indicate that there are no significant modifications in terms of reaction, which is consistent with the explanation, as crystallization does not imply a change in the proportions with which the reactants (oxalate and protons) are reacting, but rather a different non-reactive process in which water-soluble species transforms into a solid. However, this higher local concentration of oxalic acid near the membrane, in the same area where the oxalate ion transported through the membrane arrives, causes both ions to meet in a very specific zone where locally the concentration of oxalic acid will be higher, although in general terms (if not considered the concentration gradient) in the compartment it is the same as with the other membranes. It is important to consider that the saturation concentration of oxalic acid in water is 1 *M*, approximately, that it is a value far away from the concentrations measured in the compartment (89.75 and 121.13 mM, respectively for the current densities of 12.6 and 25.8 mA cm^{-2}). However, the explanation given is consistent with that of H. Strathmann [39]. The polarization caused in the medium between the feed compartment near the cathode and the product compartment near the anode, both separated by an AEM, leads to an accumulation of ions on the membrane surface on the product (concentrated) compartment side which can result in precipitation, in this case crystallization, of salts when the concentration exceeds the solubility limit of the salt, in this case a carboxylic acid. Figure SM1 shows a schematic representation of this phenomenon.

The current efficiency (CE) and the specific energy consumed (SEC) for each of the acids (OA and AA) with the studied AEMs was further calculated according to Eqs. (10) and (11) respectively:

$$\frac{NF}{I \cdot 3600} \cdot 100 \tag{10}$$

$$\frac{V \cdot I}{N} \tag{11}$$

Where, *N* is the moles of charge per hour ($molh^{-1}$), *F* is the constant of Faraday ($Cmol^{-1}$), *I* is the current intensity (*A*) and *V* is the voltage (*V*).

Table 1 shows the current efficiency and energy consumption data in the experiments. In the case of AA, the CE is very similar in all cases with a value of about 29–34 %. However, in the case of FAB and FAS at 12.8 $mAcm^{-2}$ the efficiency almost doubles reaching values of 58.28 % and 58.31 %, respectively. In the experiments with OA, higher CE values were obtained. These were always higher at 12.8 mA cm-2 than at 25.6 $mAcm^{-2}$, being the highest for FAA and FAB membranes. Table 1 shows that the highest EC was obtained at 25.6 $mAcm^{-2}$ for FAB (in AA and OA). However, these were the conditions in which the highest amount of OA crystals was obtained. Phase changes in the electrodialysis process can produce an increase in energy consumption [40].

Considering that the transport of acetate with the FAB membrane is not favored at high current densities and the possibility of using electrochemically assisted crystallization as an efficient method for oxalate separation, the FAB membrane clearly shows advantages compared to the other three membranes it is being compared with. For this reason, it is the membrane that will be used in the next crystallization and purification tests.

Table 1
AA and OA current efficiency and energy consumption by using de AEMs studied (AMH, FAA, FAB and FAS) under 12.8 and 25.6 $mAcm^{-2}$ of current density applied.

AEM.	J (mA cm^{-2})	AA		OA	
		CE (%)	SEC (Wh mol^{-1})	CE (%)	SEC (Wh mol^{-1})
AMH	12.8	29.31	642.92	52.97	376.48
AMH	25.6	34.26	890.44	44.88	729.87
FAA	12.8	34.34	491.78	69.65	270.55
FAA	25.6	31.57	825.35	43.65	778.08
FAB	12.8	58.28	342.64	64.60	324.93
FAB	25.6	29.15	1043.59	37.03	1009.07
FAS	12.8	58.31	334.22	52.08	363.91
FAS	25.6	32.61	816.27	52.37	558.92

3.2. Characterization of the electrochemically assisted crystallization

Initially, oxalate crystallization could be seen as a problem, but it can become an important opportunity from a treatment perspective, as it favors the removal of oxalate in the form of crystals, which can be very interesting from the perspective of valorizing this carboxylic acid due to the ease of separation of these types of solids. This importance increases considering that while acetic acid is the most frequently produced carboxylic acid in biological oxidation processes, oxalic acid is the main compound in chemical and electrochemical oxidation (including radical processes encompassed in the concept of advanced oxidation) [15,30], which adds value within the electro-refinery concept we are currently developing. In this context, to characterize the electrochemically assisted crystallization process in more detail, a series of additional tests with longer duration were conducted at higher pH and a larger current density range, as it was expected that increases in both variables would lead the crystallization process more effective. Additionally, only the FAB membrane was used as it demonstrated the best results for this process, a situation reflected not only in the fact that it was greater than with the other membranes but also that this electrochemically assisted crystallization occurred even at a current density of 12.5 mA cm^{-2}.

The OA content (mmol) in the feed compartment and OA crystals generated (calculated) over the time are shown in the Fig. 8, where it is observed that the crystal formation rate increases significantly with current density. It is important to highlight that during these experiments, the presence of oxalic acid crystals was observed in the tank associated to the product compartment, but these crystals were only quantified at the end of the corresponding experiment because the cell was not opened until that moment. As a result, as mentioned in the previous section, the crystals generated during the tests were not quantified by weighting, but from the concentrations of oxalic acid in the feed and product compartments, that allows to calculate the amount of oxalic acid that is not soluble and therefore crystallized. Therefore, crystallization of oxalic acid was not visually confirmed until enough crystals were released from the membrane to be visible in the product tank. The time at which this occurred was different depending on the current density applied. In the absence of applied current, no oxalic acid crystals were observed. In the case of 12.5 $mAcm^{-2}$ of current density applied, crystals began to be detectable to the naked eye after 15 *h* of experiment. In the case of 25.0 $mAcm^{-2}$ crystals were visible after 10 *h* and in the case of 37.5 $mAcm^{-2}$ were visible after 8 *h*. After these times, a massive crystallization process was observed, and the crystals were deposited at the bottom of the product recirculation tank.

For each of the tests, it is observed that after an initial period, the amount of crystals increases significantly. This initial time is more clearly observed in the low current density test and may correspond to the initial nucleation of the crystals, which justifies its dependence on the initial concentration. Therefore, after 10 h of running the experiments (value arbitrarily selected to compare all current densities) the total amount of oxalic acid crystals collected in the product compartment were: 8.0 *mmol* (719.8 *mg*), 18.9 *mmol* (1704.2 *mg*) and 25.2 *mmol* (2273.6 *mg*) for 12.5, 25.0 and 37.5 $mAcm^{-2}$ respectively. No crystals were observed in the absence of current density. Values shown in Fig. 8b are the result of the calculation from mass balance between OA analyzed in feed and product compartment and these values could be considered experimental error due to its low value (near to 0 mmol). However, this formation is occurring at average concentration values of 168.6, 144.8 and 137.2 *mM* of oxalic acid in the aqueous phase for 12.5, 25.0 and 37.5 $mAcm^{-2}$ respectively, values that are considerably below the saturation concentration of oxalic acid in water which is 1 *M*, aproximately. Again,

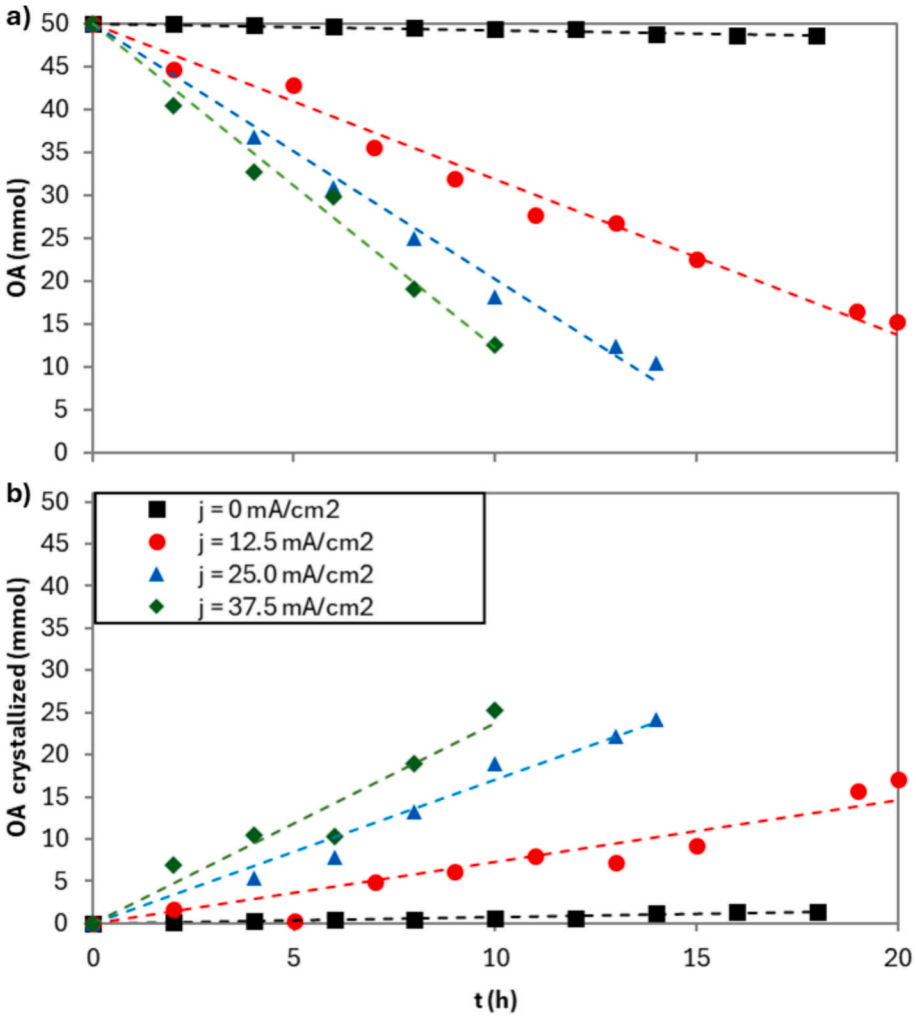

Fig. 8. a) Molar content (*mmol*) of oxalic acid solved in the feed compartment b) calculated crystallized oxalic acid at different current densities: 0 $mAcm^{-2}$, 12.5 $mAcm^{-2}$, 25 $mAcm^{-2}$ and 37.5 $mAcm^{-2}$. Symbols represent the experimental results and lines represent linear fitting.

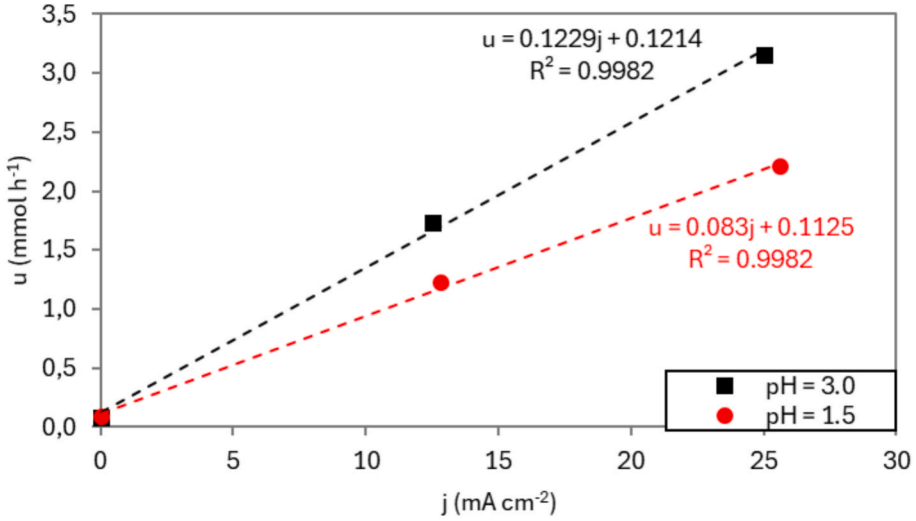

Fig. 9. Influence of the current density and pH in the feed solution on the carboxylate transport rate. Squares from stream purification experiments (pH 3.0) and circles from selection of AEM experiments (pH 1.5). All tests are carried out using FAB as AEM. Symbols represent experimental results and lines represent linear fitting.

this can be explained by the local increase in the oxalic acid concentration in the nearness of the FAB (AEM) surface, which results in a concentration higher than the solubility limit of oxalic acid in water (1 *M*, approximately) as proposed by H. Strathmann [39].

The formation of crystals could also be explained by exceeding the current density limit of the system. Figure SM3 shows the current density results obtained at different voltages. This figure shows how for all systems (AMH, FAA, FAB and FAS) the current density increases steadily with voltage without reaching a limit value. The maximum voltage value used (30 V) and the associated current density (39.8 for FAB) were considerably higher than those used in the crystallization experiments. Therefore, in the voltage range used in the cell there are no limitations associated with the transit of ions through the anionic membrane. If there were a limitation, the intensity would simply not have increased with increasing voltage.

In all cases, the experiments were left for a sufficient time to reduce the oxalic acid concentration by 80 % in the feed stream, and it is seen that for the two experiments conducted at higher current density, 50 % transformation into crystals is achieved, with the remaining 30 % in the acid product solution, with a time to achieve this change that is slightly shorter in the higher current density test (10 h versus 15 h). However, in terms of electric charges passed, the charge passed is practically the same in both cases (2.34 *Ah*), being significantly higher than the charge passed after 20 h in the experiment conducted at 12.5 mA cm^{-2} (1.56 *Ah*), which justifies that in that case, although 80 % of the oxalate in the feed solution was also separated, the crystallization is somewhat lower (36 %).

Fig. 9 shows a comparison of the molar migration rates of oxalic acid measured in these series of tests carried out at two different pHs (1.5 and 3) in the feed compartment. As can be observed, the ion transport rate increases linearly in both cases with the applied current density. However, the values of this rate are much higher in the tests where the feed is at a pH of 3.0, due to the greater presence of dissociated species (oxalates and bioxalates) compared to non-dissociated species (oxalic acid). It is important to mention that at pH 3.0 the amount of sulfate ions is lower than at 1.5 (due to the addition of H2SO4 for pH adjustment), which could allow a greater transfer of anions derived from oxalic acid. However, the effect of the presence of sulfate anions has not been studied in this work. The ratio between rates, given by the relationship between the slopes, is 0.688 (0.0827 mmol cm^2 $mA^{-1}h^{-1}$ versus 0.1229 mmol cm^2 $mA^{-1}h^{-1}$ in the case of pHs 1.5 and 3.0, respectively) and is consistent with the expected ratio with this higher proportion of dissociated species (66.14 % at pH 1.5 and 98.49 % at pH 3.0), which keeps almost the same ratio (0.671 times), pointing out the importance of this dissociation in the rate of the carboxylates transport through the FAB AEM.

Finally, the specific energy consumption was calculated for oxalic acid concentration. In the 12.5 $mAcm^{-2}$ experiment, a product concentration of 183.06 *mM* was achieved after 20 h at a rate of 550.47 $Whmol^{-1}$ (6.12 $kWhkg^{-1}$). In the experiment at 25.0 $mAcm^{-2}$ a concentration of 160.35 *mM* was obtained after 14 h at a rate of 1032.61 $Whmol^{-1}$ (11.47 $kWhkg^{-1}$) and finally in the experiment at 37.5 $mAcm^{-2}$ a product concentration of 130.40 *mM* was obtained after 10 h of experiment, which represented a cost of 1581.87 $Whmol^{-1}$ (17.58 $kWhkg^{-1}$). Current efficiencies were 59.48 %, 54.14 % and 41.52 % for 12.5 $mAcm^{-2}$, 25.0 $mAcm^{-2}$ and 37.5 $mAcm^{-2}$, respectively. Z.X. Wang et al. [41], for the recovery by electrodialysis (very similar system but without CEMs) of carboxylic acids from cyclohexanone manufacturing waste streams (among which oxalic acid is found) obtained a consumption between 3.9—22.8 $kWhkg^{-1}$ with an energy efficiency between 20.8 % and 42.1 %. Regarding pilot scale works, F. Alvarez et al. [42], obtained consumptions of 15–20 $kWhkg^{-1}$ for the recovery of salicylic acid up to a product concentration of 4.5 gL^{-1} with a efficiency of 80–90 %. These values are very similar to those obtained for OA concentration in this work. However, even if the feed solution is concentrated, crystallization of the target acids has not been observed.

3.3. Stream purification

Although initially it was expected that pH regulation would achieve changes enabling effective separation of acetate and oxalate in solutions containing both components, the results of the characterization of the transport of both components through the membranes have not been very encouraging regarding the use of this strategy. This is because the transport of acetate through the membranes is significant, being comparable to that of oxalate under the same conditions, regardless of whether the prevailing species in the feed compartment is molecular or ionic. On the other hand, the possibility of achieving oxalate crystallization is an important advantage, although this crystallization occurs in the product compartment. For this reason, two pH conditions in the feed compartment were selected to carry out the separation of both carboxylates and experiments were conducted at pHs 0.6 and 1.5. In the first case, to see the effect concerning the first dissociation of oxalic acid and in the second case concerning the second dissociation. The results obtained are shown in Fig. 10, where it can be observed how pH significantly influences both the transport rate of each species and the achieved separation.

Considering the pKa values, at pH 0.6, the proportion between acetic acid and acetate concentrations is 99.993 to 0.007 %, meaning that the amount of ionized compound is practically negligible. In the case of oxalic acid-derived species, the proportion at this pH is 80.827 % oxalic acid, 19.708 % bioxalate, and 0.005 % oxalate. This means that the amount of ionized compound is around only one-fifth of the total content in the mixture, and the concentration of the double ionized species is insignificant. Under these conditions, it is observed that the transfer rate is lower than in the case at pH 1.5. In addition, the presence of a higher amount of sulfate ions (due to the addition of H2SO4 for pH adjustment) could also be limiting the migration of organic anions from oxalic and acetic acid. However, can be observed that the compound obtained in the acid product compartment (near the anode compartment of the cell) is practically pure bioxalate, with practically no acetic-derived species detected. As a result, the solution in the cathode compartment is becoming enriched with this compound (acetic acid) over time. Thus, acetic acid molar fraction was increasing in feed compartment until 0.54.

In the test conducted at pH 1.5, the proportions between species vary substantially in the initial solution. Thus, the initial composition of species derived from acetic acid is 99.945 % of acetic acid compared to 0.055 % acetate, with the presence of these ionized species again being practically negligible. This is not the case for the other compound present in the mixture, where the proportion of oxalic acid is 33.857 % and the proportion of ionized species is much higher, with 66.017 % of bioxalate and 0.126 % of oxalate.

The Fig. 11 represent the influence of pH on carboxylate transport rate through the FAB AEM. The increase in the presence of ions is associated with a notable increase in the ion transport rate [38], as reflected in Fig. 11, being 3.23 times greater than that measured at pH 0.6 for oxalic acid-derived species but very similar to the rate obtained in the tests where the performance of the membranes was evaluated. The same occurs for acetic acid although in this case transport is negligible at pH 0.6. The molar ratio of acetic acid increased in the feed compartment from 0.50 at the beginning of the experiment to 0.56 after 6 *h* oxalic acid evolved inversely to acetic acid. The mole ratio of oxalic acid was continuously decreasing until it reached a value of 0.44 at the end of the experiment. However, the increase in the mole fraction of acetic acid does not mean that the compound was concentrated in the feed. As can be seen in Fig. 10, the total amount of each of the acids decreased over time due to migration from the feed compartment to the product. Observing the evolution of acetic acid and oxalic acid in the product compartment, the mole fraction values for each acid remain constant (0.40 and 0.60 for acetic and oxalic acids, respectively). Therefore, it can

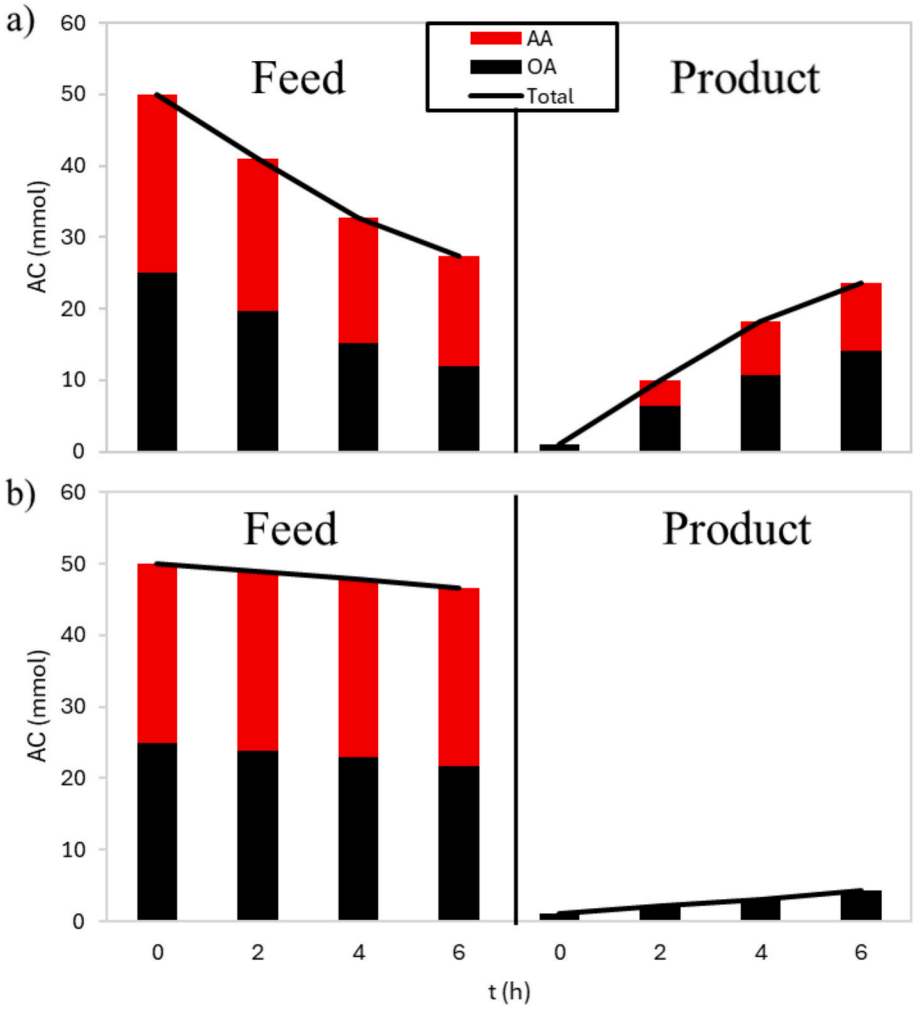

Fig. 10. Total amount of oxalic and acetic acids (*mmol*) in the feed and product compartments at pH a) 1.5 and b) 0.6 at 25.6 $mAcm^{-2}$ of current density applied. The data for the feed compartment is shown on the left and the product on the right.

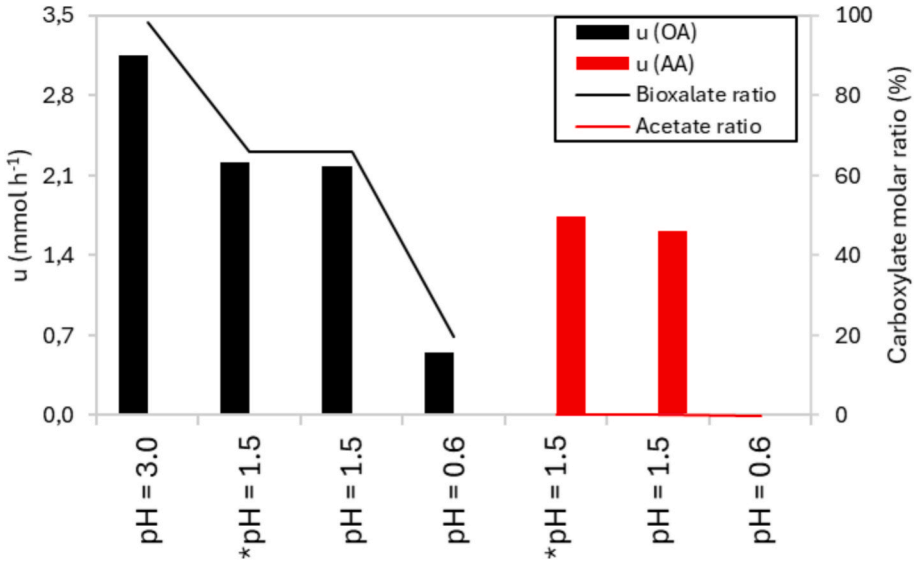

Fig. 11. Influence of pH on carboxylate transport rate through the FAB AEM. Bars represent experimental values of oxalic and acetic acids migration rates in the tests made (from left to right) with pure oxalic acid feed solution at pH 3.0, with pure oxalic or acetic acid feed solutions at (*) pH 1.5 and mixed carboxylic acid solutions at pH 1.5 and 0.6 under application of constant current density of 25.6 $mAcm^{-2}$ (at pH 3 the current density was 25.0 $mAcm^{-2}$). Lines represent carboxylate molar ratio (bioxalate and acetate) for the different experiments carried out at constant current density of 25.6 $mAcm^{-2}$ (at pH 3 the current density was 25.0 $mAcm^{-2}$).

be concluded that if the conditions of the experiment are maintained for enough time, an aqueous solution could be obtained in the feed compartment containing only acetic acid. However, the concentration of acetic acid would be considerably lower than the initial one. In addition, a slightly oxalic acid-enriched stream would be obtained in the product compartment. At pH 1.5 a total of 13.0 *mmol* of oxalic acid migrated, however, at pH 0.6 only 3.35 *mmol* of oxalic acid were obtained after 6 *h* of experiment (a reduction of 74.3 %.). Fig. 11 also shows that the transport rate depends on the ionization of oxalic acid, and, in fact, a linear relationship is observed (Figure SM2) for the oxalic acid case.

A last important observation is related to crystallization that is only observed in the test in which the feed had an initial pH of 1.5, pointing out that it is necessary that an important amount of oxalate reaches the other face of the membrane. The bioxalate transport rates increase linearly with pH and affect separation and crystallization.

4. Conclusions

In this work a study has been carried out with the main objective of studying the feasibility of a purification process of organic acids by means of electrodialysis by pH control. Within the framework of electrorefinery, two of the acids that can be obtained mainly in the oxidative degradation of organic matter have been selected.

The transport of acetate and oxalate by electrodialysis using anion exchange membranes AMH, FAA, FAB, or FAS is feasible. pH 1.5 (between the OA and AA pKa) allowed a considerably higher ionization of oxalic acid compared to acetic acid. This resulted in OA migration being favored over AA migration through the AEMs. Furthermore, it was observed that the transport velocities of the species were significantly dependent on the AEM used. Diffusion migration velocities (in the absence of electric field) were negligible compared to the velocities obtained at the current densities studied. It was observed that the FAB membrane obtained a high migration speed of OA in addition to the highest production of OA crystals.

Electrodialysis with the FAB membrane leads to the generation of oxalic acid crystals, with this electrochemically assisted crystallization process being very interesting for the effective separation of this component. This is because it does not significantly affect the process operation, as the crystals are effectively removed from the membrane surface by the shear stress generated by the electrolyte current itself, due to the special mechanical design of the cell.

Finally, the separation of oxalate and acetate from mixtures of both components using the electrodialysis cell proposed in this work with the FAB membrane is feasible by modifying the pH to favor an adequate distribution of dissociated ionized species/protonated molecular species, as the pKa of acetic and oxalic acids are sufficiently separated. Specifically, a pure current in OA was obtained when using a pH of 0.6. However, this decrease in operating pH significantly affected the migration rate of OA, resulting in a 74.3 % reduction compared to a pH of 1.5. However, although the viability of this technology has been proven, deeper studies will be necessary to establish the key parameters to establish this as an efficient technology.

Declaration of Generative AI and AI-assisted technologies in the writing process

During the preparation of this work the authors used Co-Pilot in order to improve English and readibility. After using this tool/service, the authors reviewed and edited the content as needed and take full responsibility for the content of the publication.

CRediT authorship contribution statement

M. Richa: Investigation, Data curation, Writing – original draft, Formal analysis. **R. García-Cervilla:** Writing – original draft, Data curation, Investigation. **J. Lobato:** Validation, Writing – review & editing, Supervision. **P. Cañizares:** Writing – review & editing, Supervision, Validation. **M.A. Rodrigo:** Writing – review & editing, Supervision, Funding acquisition, Validation, Project administration, Conceptualization.

Declaration of competing interest

The authors declare that they have no known competing financial interests or personal relationships that could have appeared to influence the work reported in this paper.

Acknowledgements

This work is part of the research project PID2022-138401OB-I00 funded by MCIN/AEI/Spain and "Union Europea Next Generation EU/PRTR". Maya Richa is acknowledged for the FPI grant. PREP2022-000324 to the Spanish Government. Raúl García Cervilla is acknowledged to the Spanish Government for the Juan de la Cierva postdoctoral grant. (JDC2022-049619-I).

Appendix A. Supplementary data

Supplementary data to this article can be found online at https://doi.org/10.1016/j.seppur.2025.134073.

Data availability

Data will be made available on request.

References

[1] M. Ahmaruzzaman, Role of fly ash in the removal of organic pollutants from wastewater, Energy Fuel 23 (3–4) (2009) 1494–1511, https://doi.org/10.1021/ef8002697.
[2] D. Ghime, P. Ghosh, Removal of organic compounds found in the wastewater through electrochemical advanced oxidation processes: a review, Russ. J. Electrochem. 55 (7) (2019) 591–620, https://doi.org/10.1134/s1023193519050057.
[3] P. Gururani, P. Bhatnagar, V. Kumar, M.S. Vlaskin, A.V. Grigorenko, Algal consortiums: a novel and integrated approach for wastewater treatment, Water 14 (22) (2022) 3784, https://doi.org/10.3390/w14223784.
[4] V.A. Kolesnikov, V.I. Il'in, A.V. Kolesnikov, Electroflotation in wastewater treatment from oil products, dyes, surfactants, ligands, and biological pollutants: a review, Theor. Found. Chem. Eng. 53 (2) (2019) 251–273, https://doi.org/10.1134/s0040579519010093.
[5] S. Lim, J.L. Shi, U. von Gunten, D.L. McCurry, Ozonation of organic compounds in water and wastewater: a critical review, Water Research 213 (2022) 118053, https://doi.org/10.1016/j.watres.2022.118053.
[6] R. Garcia-Cervilla, A. Santos, A. Romero, D. Lorenzo, Remediation of soil contaminated by lindane wastes using alkaline activated persulfate: kinetic model, Chem. Eng. J. 393 (2020) 124646, https://doi.org/10.1016/j.cej.2020.124646.
[7] R. Garcia-Cervilla, A. Santos, A. Romero, D. Lorenzo, Abatement of chlorobenzenes in aqueous phase by persulfate activated by alkali enhanced by surfactant addition, J. Environ. Manag. 306 (15) (2022) 114475, https://doi.org/10.1016/j.jenvman.2022.114475.
[8] C.A. Martinez-Huitle, M.A. Rodrigo, I. Sires, O. Scialdone, A critical review on latest innovations and future challenges of electrochemical technology for the abatement of organics in water, Appl. Catal. B-Environ. 328 (2023) 122430, https://doi.org/10.1016/j.apcatb.2023.122430.
[9] G. Divyapriya, S. Singh, C.A. Martinez-Huitle, J. Scaria, A.V. Karim, P.V. Nidheesh, Treatment of real wastewater by photoelectrochemical methods: an overview, Chemosphere 276 (2021) 130188, https://doi.org/10.1016/j.chemosphere.2021.130188.
[10] A. Moiseev, H. Schroeder, M. Kotsarldou-Nagel, S.U. Geissen, A. Vogelpohl, Photocatalytical polishing of paper-mill effluents, Water Sci. Technol. 49 (4) (2004) 325–330, https://doi.org/10.2166/wst.2004.0296.
[11] J.H. Zhang, Study on treatment of organic wastewater by chemical oxidation technology, Dissertation/Thesis Jan 01 2008. [Online]. Available: <Go to ISI>://PQDT:67257621.
[12] P. Ritesh, V.C. Srivastava, Understanding of ultrasound enhanced electrochemical oxidation of persistent organic pollutants, J. Water Process Eng. 37 (2020) 101378, https://doi.org/10.1016/j.jwpe.2020.101378.
[13] M. Loizidou, Waste valorization and management, Waste Biomass Valoriz. 7 (4) (2016) 645–648, https://doi.org/10.1007/s12649-016-9630-1. Editorial Material.
[14] P.T.T. Nguyen, et al., Recent progresses in eco-friendly fabrication and applications of sustainable aerogels from various waste materials, Waste Biomass Valoriz. 13 (4) (2022) 1825–1847, https://doi.org/10.1007/s12649-021-01627-3.

[15] R.S.S. Castro, et al., New MMO coatings for electro-refinery applications: promoting the production of carboxylates, Chemosphere 363 (2024) 142941, https://doi.org/10.1016/j.chemosphere.2024.142941.
[16] L. Bartolucci, et al., Sustainable valorization of bioplastic waste: a review on effective recycling routes for the most widely used biopolymers, Int. J. Mol. Sci. 24 (9) (2023) 7696, https://doi.org/10.3390/ijms24097696.
[17] D. Buchanan, W. Martindale, E. Romeih, E. Hebishy, Recent advances in whey processing and valorisation: Technological and environmental perspectives, Int. J. Dairy Technol. 76 (2) (2023) 291–312, https://doi.org/10.1111/1471-0307.12935.
[18] G.D. Gebreeyessus, Towards the sustainable and circular bioeconomy: insights on spent coffee grounds valorization, Sci. Total Environ. 833 (2022), https://doi.org/10.1016/j.scitotenv.2022.155113.
[19] D. Spagnuolo, et al., Conventional vs. innovative protocols for the extraction of polysaccharides from macroalgae, Sustainability 14 (10) (2022) 5750, https://doi.org/10.3390/su14105750.
[20] C. Huang, T. Xu, Y. Zhang, Y. Xue, G. Chen, Application of electrodialysis to the production of organic acids: state-of-the-art and recent developments, J. Membr. Sci. 288 (1–2) (2007) 1–12, https://doi.org/10.1016/j.memsci.2006.11.026.
[21] C. Carlesi Jara, D. Fino, Cost optimization of the current density for electroxidation wastewater processes, Chem. Eng. J. 160 (2) (2010) 497–502, https://doi.org/10.1016/j.cej.2010.03.060.
[22] M. Bullmann, et al., Tailored PEO synthesis and in-situ ATR-FTIR study of PtSnO 2 /Nb coral-like structures for application in ethanol electrooxidation, J. Alloy. Compd. 1002 (2024) 175178, https://doi.org/10.1016/j.jallcom.2024.175178.
[23] X. Zhao, J. Li, J. Zhang, J.-H. Yang, Urea electrooxidation: research progress and application of supported nickel-based catalysts, Ionics 29 (8) (2023) 2969–2987, https://doi.org/10.1007/s11581-023-05107-7.
[24] Y. Zhu, J. Wei, J. Wu, R. Chen, P. Tsiakaras, S. Yin, Built-in electric field in NiO-CuO heterostructures to regulate the hydroxide adsorption sites for 5-hydroxymethylfurfural electrooxidation assisted hydrogen production, J. Colloid Interface Sci. 673 (2024) 301–311, https://doi.org/10.1016/j.jcis.2024.05.216.
[25] R. Granados-Fernandez, M.A. Montiel, C.M. Fernandez-Marchante, J. Lobato, M. A. Rodrigo, Tailoring electrochemically assisted absorbers for the efficient removal of volatile organic compounds, J. Environ. Chem. Eng. 12 (1) (2024), https://doi.org/10.1016/j.jece.2023.111620. 111620.
[26] S.O. Ganiyu, C.A. Martinez-Huitle, M.A. Rodrigo, Renewable energies driven electrochemical wastewater/soil decontamination technologies: a critical review of fundamental concepts and applications, Appl. Catal. B-Environ. 270 (2020) 118857, https://doi.org/10.1016/j.apcatb.2020.118857.
[27] B.E. Logan, Simultaneous wastewater treatment and biological electricity generation, Water Sci. Technol. 52 (1–2) (2005) 31–37, https://doi.org/10.2166/wst.2005.0495. Proceedings Paper.
[28] F.L. Souza, C. Saez, J. Llanos, M.R.V. Lanza, P. Canizares, M.A. Rodrigo, Solar-powered CDEO for the treatment of wastewater polluted with the herbicide 2,4-D, Chem. Eng. J. 277 (2015) 64–69, https://doi.org/10.1016/j.cej.2015.04.118.
[29] E.V. dos Santos, C.A. Martinez-Huitle, M.A. Rodrigo, The electro-refinery in organics: a new arising concept for valorization of wastes, Curr. Opin. Electrochem. 39 (2023) 101267, https://doi.org/10.1016/j.coelec.2023.101267.
[30] H.L. Oliveira, et al., Electrochemical oxidation of a real effluent using selective cathodic and anodic strategies to simultaneously produce high value-added compounds: green hydrogen and carboxylic acids, Electrochem. Commun. 154 (2023) 107553, https://doi.org/10.1016/j.elecom.2023.107553.
[31] A. Chandra, J.G.D. Tadimeti, E. Bhuvanesh, D. Pathiwada, S. Chattopadhyay, Switching selectivity of carboxylic acids and associated physico-chemical changes with pH during electrodialysis of ternary mixtures, Sep. Purif. Technol. 193 (2018) 327–344, https://doi.org/10.1016/j.seppur.2017.10.048.
[32] P. Mandal, R. Mondal, P. Goel, E. Bhuvanesh, U. Chatterjee, S. Chattopadhyay, Selective recovery of carboxylic acid through PVDF blended anion exchange membranes using electrodialysis, Sep. Purif. Technol. 292 (2022) 121069, https://doi.org/10.1016/j.seppur.2022.121069.
[33] M.C. Medeiros, E.V. dos Santos, C.A. Martinez-Huitle, A.S. Fajardo, S.S.L. Castro, Obtaining high-added value products from the technical cashew-nut shell liquid using electrochemical oxidation with BDD anodes, Sep. Purif. Technol. 250 (2020) 117099, https://doi.org/10.1016/j.seppur.2020.117099.
[34] M. Tucci, et al., Syntrophy drives the microbial electrochemical oxidation of toluene in a continuous-flow “bioelectric well”, J. Environ. Chem. Eng. 10 (3) (2022) 107799 https://doi.org/10.1016/j.jece.2022.107799.
[35] Y.X. Wu, S.A. Banwart, S.F. Thornton, D.N. Lerner, Microbial production of fatty acids in phenol-contaminated groundwater and its significance in subsurface bioremediation. in 3rd International Conference on Groundwater Quality, Sheffield, England, 2002 Jun 18-21 2001, in IAHS Publication, 2002, pp. 219-224. [Online]. Available: <Go to ISI>://WOS:000185215100034. [Online]. Available: <Go to ISI>://WOS:000185215100034.
[36] H. Park, K.-H. Choo, H.-S. Park, J. Choi, M.R. Hoffmann, Electrochemical oxidation and microfiltration of municipal wastewater with simultaneous hydrogen production: Influence of organic and particulate matter, Chem. Eng. J. 215 (2013) 802–810, https://doi.org/10.1016/j.cej.2012.11.075.
[37] T.O. Silva, R. Granados-Fernández, J. Lobato, M.R.V. Lanza, M.A. Rodrigo, Boosting new electrochemical reactor designs to improve the performance in H_2O_2 production using gas diffusion electrodes, ACS Sustain. Chem. Eng. 13 (8) (2025) 3172–3182, https://doi.org/10.1021/acssuschemeng.4c08826.
[38] A. Chandra, J.G.D. Tadimeti, S. Chattopadhyay, Transport hindrances with electrodialytic recovery of citric acid from solution of strong electrolytes, Chin. J. Chem. Eng. 26 (2) (2018) 278–292, https://doi.org/10.1016/j.cjche.2017.05.010.
[39] H. Strathmann, Electrodialysis, a mature technology with a multitude of new applications, Desalination 264 (3) (2010) 268–288.
[40] R.K. Nagarale, G.S. Gohil, V.K. Shahi, G.S. Trivedi, S.K. Thampy, R. Rangarajan, Studies on transport properties of short chain aliphatic carboxylic acids in electrodialytic separation, Desalination 171 (2) (2005) 195–204, https://doi.org/10.1016/j.desal.2004.06.190.
[41] Z.X. Wang, Y.B. Luo, P. Yu, Recovery of organic acids from waste salt solutions derived from the manufacture of cyclohexanone by electrodialysis, J. Membr. Sci. 280 (1–2) (2006) 134–137, https://doi.org/10.1016/j.memsci.2006.01.015.
[42] F. Alvarez, R. Alvarez, J. Coca, J. Sandeaux, R. Sandeaux, C. Gavach, Salicylic acid production by electrodialysis with bipolar membranes, J. Membr. Sci. 123 (1) (1997) 61–69, https://doi.org/10.1016/s0376-7388(96)00197-4.